our model *A*12, attempts to refine structures using such overlapping powder data leads to the situation where the refined model becomes completely dependent on the starting model. Our comparative testing of the various models, described earlier, helped us to avoid any such false refinement minima.

4. Summary and discussion

Like its octahedral corner-connected perovskite counterpart (Barnighausen, 1980), the *C*9 structure type represents an ideal parent structure or aristotype from which many lower symmetry derivative structures can be obtained *via* appropriate rotation of more or less rigid framework polyhedra (tetrahedral in the case of *C*9-related structures and octahedral in the case of perovskite-related structures). Given that one of the major objectives of crystal chemistry is the interrelationship between such cognate crystal structures, it is important not only to solve for the crystal structure of low carnegieite but also to place it in relationship to its underlying *C*9 aristotype. The use of a modulation wave approach to the structural parameterization and refinement of low carnegieite not only spelt out this relationship in detail but also made clear that there is more than one plausible starting model compatible with rigid-body rotation of the tetrahedral framework. Such an approach allowed for the systematic testing of alternative possibilities and hence avoided any problems associated with false refinement minima. It also provided plausible and essential starting models for the subsequent full Rietveld refinement.

Topologically the coupled tetrahedral edge rotations which generate the structure of low carnegieite from its underlying *C*9 aristotype have *Pbca* space-group symmetry (for our choice of cell setting) and in this sense the structure of low carnegieite is closely related to those of $KGaO_2$ (Vielhaber & Hoppe, 1969) and $Na_{1-x}[Fe_{1-x}Si_x]O_2$ (Grey *et al.*, 1990). The major difference and the origin of the reduction in space group symmetry from *Pbca* to $Pb2_1a$ in the case of low carnegieite arises from the difference in the ordering of the tetrahedral and stuffing cations. In the case of low carnegieite, the Al/Si and Na/vacancy ordering corresponds to a $\mathbf{q} = 0$ compositional modulation of its underlying *C*9 aristotype whereas, in the case of $Na_{1-x}[Fe_{1-x}Si_x]O_2$, the Fe/Si and Na/vacancy ordering require a $\mathbf{q} = \mathbf{b}^*$ compositional modulation.

References

BARNIGHAUSEN, H. (1980). *Commun. Math. Chem.* **9**, 139-175.

BRADLEY, C. J. & CRACKNELL, A. P. (1972). *The Mathematical Theory of Symmetry in Solids*, p. 118. London: Oxford Univ. Press.

BRESE, N. E. & O'KEEFFE, M. (1991). *Acta Cryst.* B**47**, 192-197.

BROWN, I. D. & ALTERMATT, D. (1985). *Acta Cryst.* B**41**, 244-247.

FORIS, C. M., ZUMSTEG, F. C. & SHANNON, R. D. (1979). *J. Appl. Cryst.* **12**, 405-406.

GREY, I. E., HOSKINS, B. F. & MADSEN, I. C. (1990). *J. Solid State Chem.* **85**, 202-219.

KLINGENBERG, R. & FELSCHE, J. (1981). *J. Appl. Cryst.* **14**, 66-68.

O'KEEFFE, M. & HYDE, B. G. (1976). *Acta Cryst.* B**32**, 2923-2936.

PEREZ-MATO, J. M., MADARIAGA, G., ZUÑIGA, F. J. & GARCIA ARRIBAS, A. (1987). *Acta Cryst.* A**43**, 216-226.

SHANNON, R. D. (1979). *Phys. Chem. Miner.* **4**, 139-148.

SHELDRICK, G. M. (1976). *SHELX*76. Program for crystal structure determination. Univ. of Cambridge, England.

THOMPSON, J. G., WITHERS, R. L., WHITTAKER, A. K., TRAILL, R. M. & FITZ GERALD, J. D. (1993). *J. Solid State Chem.* In the press.

VIELHABER, E. V. & HOPPE, R. (1969). *Z. Anorg. Allg. Chem.* **369**, 14-32.

WILES, D. B. & YOUNG, R. A. (1981). *J. Appl. Cryst.* **14**, 149-151.

WITHERS, R. L., HUA, G. L., WELBERRY, T. R. & VINCENT, R. (1988). *J. Phys. C*, **21**, 309-318.

WITHERS, R. L., THOMPSON, J. G. & WELBERRY, T. R. (1989). *Phys. Chem. Miner.* **16**, 517-523.

WITHERS, R. L., WALLENBERG, R., BEVAN, D. J. M., THOMPSON, J. G. & HYDE, B. G. (1989). *J. Less Common Met.* **156**, 17-27.

YAMAMOTO, A. (1982). *Acta Cryst.* A**38**, 87-92.

Acta Cryst. (1993). B**49**, 626–631

Structure of $Ba_4Nb_{14}O_{23}$

BY G. SVENSSON AND J. GRINS

Department of Inorganic Chemistry, Arrhenius Laboratory, Stockholm University, S-106 91 Stockholm, Sweden

(*Received* 8 *January* 1993; *accepted* 24 *March* 1993)

Abstract

Single crystals of $Ba_4Nb_{14}O_{23}$ were obtained by heat treatment of a pelleted mixture of $Ba_5Nb_4O_{15}$, Nb_2O_5 and Nb at 1725 K in an Ar atmosphere. High-resolution electron microscopy studies showed the structure to be an intergrowth of the $BaNbO_3$ perovskite structure and the NbO structure. The structure model was refined using X-ray single-crystal diffraction data. Characteristic structural units are triple chains of corner-sharing Nb_6 octahedra, parallel to the *c* axis and separated by perovskite-type columns. Crystal data: barium oxoniobate, $Ba_4Nb_{14}O_{23}$, M_r = 2218.0, orthorhombic, *Cmmm*, $a = 20.79\,(1)$, $b =$

12.453 (6), $c = 4.149$ (1) Å, $V = 1074$ (1) Å^3, $Z = 2$, $D_x = 6.86$ g cm^{-3}, λ(Cu $K\alpha$) = 1.5418 Å, $F(000) = 1964$, $T = 295$ K, $R = 0.031$ for 419 observed unique reflections.

Introduction

A number of phases in the BaO—NbO—NbO_2 system have intergrowth-type structures composed of $BaNbO_3$ (perovskite-type) and NbO (ordered deficient NaCl-type) elements. The structure of $Ba_{0.95}NbO_3$ ($BaNbO_3$ with partly occupied Ba positions: Kreiser & Ward, 1970; Hessen, Sunshine, Siegrist & Jimenez, 1991) exhibits a framework of corner-sharing NbO_6 octahedra. The Ba atoms are located in the cubo-octahedra formed by the O atoms. The structure of NbO (Brauer, 1941) is usually described as an ordered deficient NaCl-type structure, with a quarter of both anion and cation positions vacant. The Nb atoms form a framework of corner-sharing Nb_6 octahedra similar to that formed by the NbO_6 octahedra in $BaNbO_3$. Alternatively, however, the structure can be described in terms of three-dimensionally condensed Nb_6O_{12} clusters (Schäfer & Schnering, 1964), each cluster constituting the atomic arrangement of an isolated cubic NbO unit cell.

A number of known barium oxoniobate intergrowth structures are illustrated in Fig. 1. They exhibit Nb_6O_{12} clusters, which are condensed in one or two dimensions. Lamellar structures, with Nb_6O_{12} clusters condensed in two dimensions, are found in several barium oxoniobates (Köhler, Svensson & Simon, 1992). The structure of $BaNb_4O_6$ (Zubkov, Perelyaev, Berger, Voronin *et al.*, 1990; Svensson, Köhler & Simon, 1991), consists of alternating NbO and $BaNbO_3$ slabs. $BaNb_7O_9$ (Svensson, Köhler & Simon, 1992*a*) has double NbO slabs alternating with single perovskite slabs. The reverse arrangement, *i.e.* single NbO slabs alternating with double perovskite slabs, is observed in $Ba_2Nb_5O_9$ (Svensson, 1988; Zubkov, Perelyaev, Berger, Voronin *et al.*, 1990; Svensson *et al.*, 1991).

Disordered one-dimensionally condensed Nb_6O_{12} clusters, forming NbO-type columns, intergrown with one-dimensional perovskite columns, were first observed in a high-resolution electron microscopy (HREM) study of barium oxoniobate samples prepared at temperatures above 1520 K (Svensson, 1990). Small regions with more ordered structures were, however, also observed. Subsequently, a number of ordered structures, exhibiting one-dimensionally condensed Nb_6O_{12} clusters, have been found in samples synthesized at higher temperatures. The structure of $BaNb_5O_8$ (Zubkov, Perelyaev, Berger, Kontsevaya *et al.*, 1990) contains single-unit perovskite columns, alternating with single-unit NbO columns. The structure of $Ba_4Nb_{17}O_{26}$ (Zubkov *et*

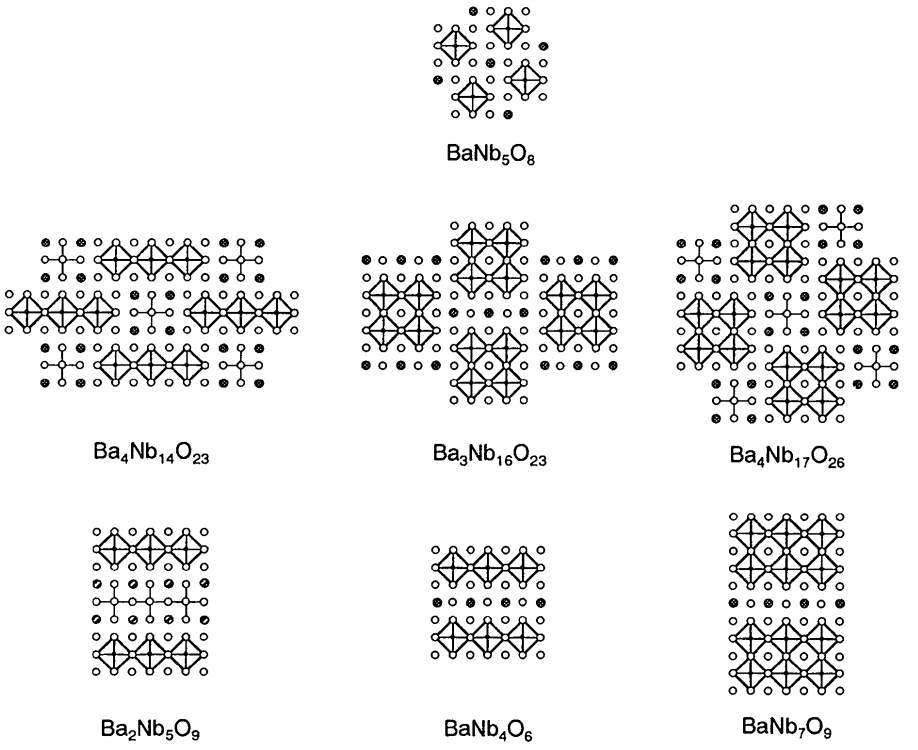

Fig. 1. Idealized intergrowth structures in the Ba–Nb–O system, viewed along their short axis. Compounds with one- and two-dimensionally condensed Nb_6O_{12} clusters are shown in the upper and lower parts of the figure, respectively. The Nb_6 octahedra in the Nb_6O_{12} clusters are outlined with bold lines and the Nb—O bonds in the perovskite NbO_6 octahedra with thin lines. Ba atoms are shown as large hatched circles, O atoms as unfilled circles and Nb atoms as small filled circles. Note that some of the Nb atoms in the Nb_6 octahedra are hidden by O atoms.

al., 1992) shows quadruple perovskite and quadruple NbO columns, and $Ba_3Nb_{16}O_{23}$ (Zubkov *et al.*, 1993) triple perovskite and quadruple NbO columns.

The approximate unrefined structure of $Ba_4Nb_{14}O_{23}$ was recently determined from HREM images and X-ray powder diffraction data (Svensson, Köhler, Otten & Simon, 1993). An HREM image of the structure together with the corresponding simulated HREM image (program suite *SHRLI*; O'Keefe, Busek & Ijima, 1978) is shown in Fig. 2. The structure of $Ba_4Nb_{14}O_{23}$ contains triple NbO columns, intergrown with quadruple perovskite columns. In the HREM image, the three corner-sharing Nb_6 octahedra in the NbO columns are seen as three dark crosses while the Ba and Nb atoms in the perovskite columns are seen as a 2.9 Å square lattice of smaller dark spots in between. The $Ba_4Nb_{14}O_{23}$ crystallites were, furthermore, found to contain defects, predominantly a variation in block size. An HREM image of an example of such a defect is shown in Fig. 3(*a*). It can be interpreted (see Fig. 3*b*) as an intergrowth of $Ba_4Nb_{17}O_{26}$ (*cf.* Fig. 1) in $Ba_4Nb_{14}O_{23}$. In order to evaluate and compare the intergrowth structures and the defects found in them, it is necessary to have accurate structural data. The present single-crystal X-ray refinement of the $Ba_4Nb_{14}O_{23}$ structure was undertaken in order to determine the atom positions more accurately, thus providing data for a more detailed comparison with other barium oxoniobate intergrowth structures.

Experimental

Synthesis

Powders of Nb_2O_5 (*p.a.* Merck), Nb (*p.a.* Merck) and $Ba_5Nb_4O_{15}$ (Roth & Waring, 1961), prepared from $BaCO_3$ (*p.a.* Merck) and Nb_2O_5 (99.9% Roth) at 1275 K, were mixed according to the composition $Ba_4Nb_{14}O_{23}$. The mixture was pelletized and placed on an Nb foil in a graphite crucible. The sample was heated in argon to 1775 K at a rate of 1000 K h^{-1}, held at 1775 K for 4 h, cooled to 1275 K at a rate of 1000 K h^{-1} and then left to cool to room temperature in the furnace. The sample obtained was grey and contained needle-shaped $Ba_4Nb_{14}O_{23}$ crystals, with lengths up to 150 μm, protruding from the pellet surface and from the Nb foil. Parts of the pellet and Nb foil had, furthermore, reacted with the graphite crucible, forming Nb carbides. X-ray powder patterns recorded with Guinier–Hägg cameras showed that

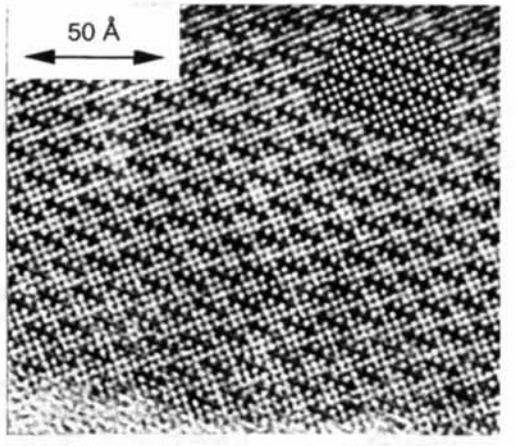

Fig. 2. HREM image of $Ba_4Nb_{14}O_{23}$ along [001] with a simulated HREM image (objective aperture 0.45 $Å^{-1}$, defocus −350 Å, 40 Å thickness) inserted. The HREM image was obtained with a Philips CM 30 electron microscope operating at 300 kV.

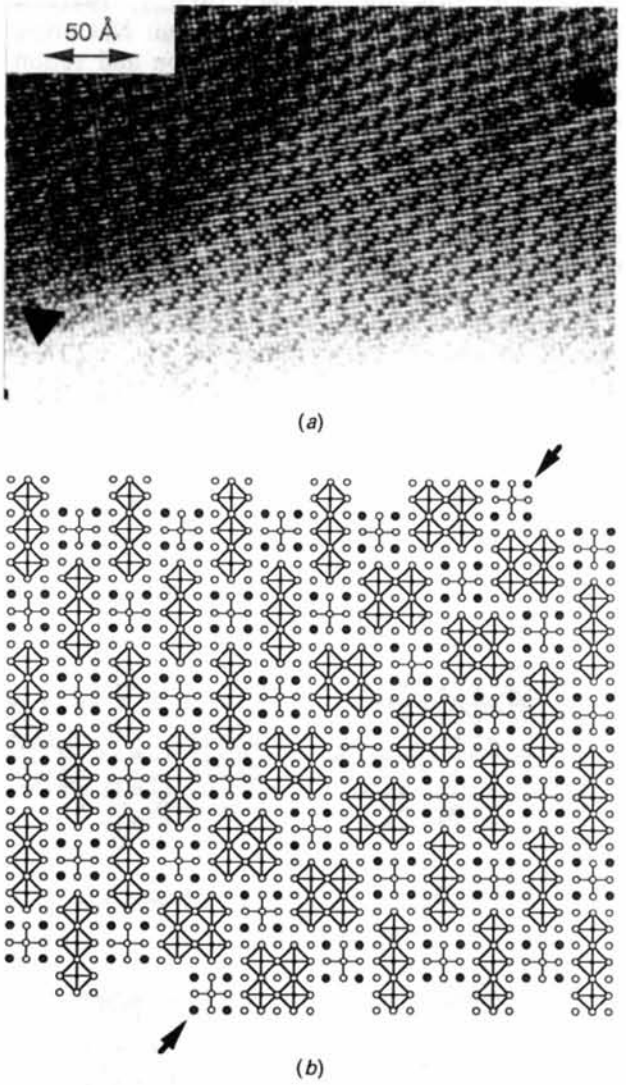

Fig. 3. (*a*) HREM image showing an intergrowth of $Ba_4Nb_{17}O_{26}$ (indicated in the image) in $Ba_4Nb_{14}O_{23}$ and (*b*) the corresponding interpretation. The HREM image was obtained with a JEOL 200CX electron microscope operating at 200 kV.

Table 1. *Crystal data of* $Ba_4Nb_{14}O_{23}$ *and experimental conditions for the crystal structure determination*

Chemical formula	$Ba_4Nb_{14}O_{23}$
Formula weight	2218.0
Space group	Orthorhombic, *Cmmm*
a (Å)	20.79 (1)
b (Å)	12.453 (6)
c (Å)	4.149 (1)
V (Å^3)	1074 (1)
Z	2
D_x (g cm^{-3})	6.86
Crystal shape/(*hkl*) (μm)	Needle prism, {001} 52; {$\bar{2}$10}, 10.9; {110}, 7.4; {310}, 9.5; {1$\bar{3}$0}, 7.7
Crystal size (mm^3)	2.7×10^{-5}
Intensity data collection	
Temperature (K)	295
λ(Cu $K\alpha$) (Å)	1.5418
F(000)	1964
Maximum $(\sin\theta)/\lambda$ (Å^{-1})	0.610
Range of h, k and l	$-25 \le h \le 25$, $0 \le k \le 15$, $0 \le l \le 5$ ($0 \le h \le 25$, $0 \le k \le 15$, $0 \le l \le 5$)*
Standard reflections	3
Intensity instability	< 1.4%
Internal R value	0.020
No. of measured reflections	1158 (601)*
No. of unique reflections	591
No. of observed unique reflections	419
Criterion for significance	$I > 3\sigma(I)$
Absorption correction	Numerical integration
Linear absorption coefficient (cm^{-1})	1182
Transmission-factor range	0.085–0.327
Structure refinement	
Minimization of	$\sum w(\Delta F)^2$
Anisotropic thermal parameters	Ba, Nb
Number of refined parameters	56
Weighting scheme	$w = 1/[\sigma^2(\lvert F\rvert) + 0.00050F^2]$
Final R	0.031
wR	0.034
wR for all reflections	0.040
Goodness of fit	1.02
$(\Delta/\sigma)_{max}$	0.003
$\Delta\rho_{min}$, $\Delta\rho_{max}$ (e Å^{-3})	−2.0, +1.3

* Data set II.

the sample contained $Ba_4Nb_{14}O_{23}$, Nb_6C_5 (Haenko & Sivak, 1990) and $Ba_6Nb_{10}O_{30}$ (Hessen, Sunshine, Siegriest, Fiory & Waszczak, 1991) as major phases.

Data collection and absorption correction

X-ray diffraction photographs, taken with de Jong and precession techniques, of a selected $Ba_4Nb_{14}O_{23}$ crystal indicated Laue symmetry *mmm* and an orthorhombic *C*-centred unit cell. X-ray diffraction data were collected on a Stoe AED-2 diffractometer; experimental conditions are listed in Table 1. Because of the small crystal size, Cu $K\alpha$ radiation was chosen to optimize reflection intensities. An initial data set was collected with the ω–2θ scan mode. The percentage of reflections with $I \ge 3\sigma(I)$ in this data set was deemed unsatisfactorily low, and a second data set was collected at a slower scan speed. In order to further improve counting statistics, the two data sets were later merged in the final refinement. Cell parameters were determined from 16 reflections in the range $30 \le 2\theta \le 50°$, yielding a = 20.787 (10), b = 12.453 (6) and c = 4.149 (2) Å, which agrees with the cell dimensions obtained from Guinier–Hägg data. The intensities were corrected for background, polarization and Lorentz effects. The crystal dimensions and the morphology were determined with a JEOL JSM-820 scanning electron microscope. Correction for absorption was then carried out by numerical Gaussian integration. The validity of the correction was checked by applying it to ψ scans of ten different reflections recorded at $56 < \chi < 73°$ and $31 < 2\theta < 112°$. The uncorrected ψ scans yielded an average R_I value of 0.26 and the corrected ones an average R_{F^2} value of 0.08.

Structure refinement

The refinements were made in space group *Cmmm* (No. 65), using *SHELX*76 (Sheldrick, 1976) and X-ray scattering factors for neutral atoms, including anomalous-dispersion terms, from *International Tables for X-ray Crystallography* (1974, Vol. IV). Starting coordinates were taken from the approximate structure model (Svensson *et al.*, 1993). In the final refinement, Ba and Nb atoms were assigned anisotropic temperature factors. Extinction effects were found to be present and an empirical extinction correction was applied with $|F_c^*| = |F_c|(1 - 10^{-4}xF_c^2/\sin\theta)$; x refined to 3.1 (2) × 10^{-4}. Atomic coordinates and temperature factors are listed in Table 2.* A previous X-ray microanalysis of $Ba_4Nb_{14}O_{23}$ indicated the possibility of a small Ba deficiency, while the present data gave no evidence for this. Selected bond lengths are given in Table 3.

Structure description and discussion

A projection of the $Ba_4Nb_{14}O_{23}$ structure on the xy plane is shown in Fig. 4. It can be described as an intergrowth of triple NbO and quadruple perovskite $BaNbO_3$ blocks. As in the NbO structure, the Nb1, Nb2, Nb3 atoms in the NbO block have a planar four-coordination of O atoms and an eight-coordination of Nb atoms, forming a tetragonal prism. The Nb4, Nb5, Nb6 atoms, completing the Nb_6 octahedra, are 4 + 1 coordinated by O atoms forming a square pyramid, and four coordinated by Nb atoms as in a discrete Nb_6O_{12} cluster, such as found in a number of reduced oxoniobates, *e.g.* $SrNb_8O_{14}$ (Köhler, Simon, Hibble & Cheetham, 1988). The O2, O3, O4, O5, O6 atoms of the square pyramids, together with the corresponding Nb4, Nb5, Nb6 atoms, are shared with the neighbouring perovskite block. In the perovskite block, the Nb7 atom is octahedrally coordinated by O atoms and the

* Lists of structure factors, anisotropic thermal parameters, and bond lengths and bond angles have been deposited with the British Library Document Supply Centre as Supplementary Publication No. SUP 71022 (17 pp.). Copies may be obtained through The Technical Editor, International Union of Crystallography, 5 Abbey Square, Chester CH1 2HU, England. [CIF reference: AB0304]

Table 2. *Fractional coordinates and isotropic thermal parameters* ($\times 10^4$)

$U_{eq} = (1/3)\sum_i \sum_j U_{ij} a_i^* a_j^* \mathbf{a}_i . \mathbf{a}_j$.

	Wyckoff position	x	y	z	U_{eq} (Å^2)
Ba	8(*p*)	1022 (1)	3303 (1)	0	86 (3)
Nb1	2(*a*)	0	0	0	50 (8)
Nb2	4(*h*)	991 (1)	0	½	50 (5)
Nb3	4(*g*)	2034 (1)	0	0	58 (6)
Nb4	4(*h*)	2981 (1)	0	½	52 (6)
Nb5	4(*j*)	0	1638 (1)	½	55 (5)
Nb6	8(*q*)	2010 (1)	1605 (1)	½	54 (4)
Nb7	2(*c*)	½	0	½	56 (8)
O1	4(*g*)	990 (10)	0	0	119 (38)
O2	4(*g*)	3048 (8)	0	0	53 (37)
O3	4(*i*)	0	1716 (13)	0	62 (36)
O4	8(*q*)	996 (6)	1703 (8)	½	106 (24)
O5	8(*p*)	1967 (5)	1675 (10)	0	131 (31)
O6	8(*q*)	3016 (5)	1655 (11)	½	126 (30)
O7	4(*h*)	4055 (8)	0	½	116 (35)
O8	2(*b*)	½	0	0	255 (76)
O9	4(*j*)	½	1616 (15)	½	116 (39)

Table 3. *Selected interatomic distances with e.s.d.'s in parentheses*

Ba—O5		2.823 (12)	Nb4—Nb6	2 ×	2.841 (2)
Ba—O2		2.864 (11)	Nb4—Nb3	2 ×	2.860 (2)
Ba—O4	2 ×	2.877 (7)	Nb4—O6	2 ×	2.062 (14)
Ba—O6	2 ×	2.882 (7)	Nb4—O2	2 ×	2.079 (1)
Ba—O3		2.902 (11)	Nb4—O7		2.233 (17)
Ba—O7	2 ×	2.966 (2)			
Ba—O9	2 ×	2.971 (2)			
Ba—O8		2.997 (2)			
Nb1—Nb5	4 ×	2.909 (1)	Nb5—Nb2	2 ×	2.899 (2)
Nb1—Nb2	4 ×	2.924 (2)	Nb5—Nb1	2 ×	2.909 (1)
Nb1—O1	2 ×	2.058 (21)	Nb5—O4	2 ×	2.072 (12)
Nb1—O3	2 ×	2.137 (16)	Nb5—O3	2 ×	2.077 (1)
			Nb5—O9		2.174 (19)
Nb2—Nb5	2 ×	2.899 (2)	Nb6—Nb4		2.841 (2)
Nb2—Nb6	2 ×	2.913 (3)	Nb6—Nb3	2 ×	2.881 (1)
Nb2—Nb1	2 ×	2.924 (2)	Nb6—Nb2		2.913 (3)
Nb2—Nb3	2 ×	3.001 (2)	Nb6—Nb6		3.020 (4)
Nb2—O1	2 ×	2.075 (1)	Nb6—O5	2 ×	2.078 (1)
Nb2—O4	2 ×	2.121 (10)	Nb6—O6		2.092 (11)
			Nb6—O4		2.112 (13)
			Nb6—O6		2.167 (14)
Nb3—Nb4	2 ×	2.860 (2)	Nb7—O7	2 ×	1.965 (17)
Nb3—Nb6	4 ×	2.881 (1)	Nb7—O9	2 ×	2.012 (19)
Nb3—Nb2	2 ×	3.001 (2)	Nb7—O8	2 ×	2.075 (1)
Nb3—O5	2 ×	2.091 (12)			
Nb3—O2		2.108 (17)			
Nb3—O1		2.170 (21)			

Ba atom surrounded by 12 O atoms, forming a cubo-octahedron. The refined single-crystal structure discussed here deviates slightly but significantly from the idealized structure reported by Svensson *et al.* (1993).

The Nb—Nb distances in the NbO blocks, 2.881 (1)–3.001 (2) Å, are similar to corresponding distances in other structures with condensed Nb_6O_{12} clusters, *e.g.* 2.977 Å in NbO (Brauer, 1941) and 2.899–2.985 Å in $BaNb_7O_9$ (Svensson *et al.*, 1992*a*). The central Nb_6 octahedron is rather regular, while the outer octahedra are somewhat distorted. The Nb2—Nb3 distance, 3.001 (2) Å, is thus significantly longer than the other Nb—Nb distances, 2.841 (2)–2.912 (3) Å. The Nb—O distances within the NbO block range between 2.06 (2) and 2.17 (2) Å. The lower limit is similar to Nb—O distances found in other oxoniobates with condensed Nb_6O_{12} clusters (Köhler *et al.*, 1992), while the longer distance is a consequence of the distortion of the outer Nb_6 octahedra. The apical Nb—O distances in the NbO_5 pyramids are longer, 2.17 (2)–2.23 (2) Å, the longest being those in which the O atoms are shared with the perovskite NbO_6 octahedra, O7 and O9. The O—Nb—O angles in the base of the NbO_5 pyramid are between 172.3 (9) and 176.0 (6)°, indicating a weak repulsion between these O atoms and the Nb_6 octahedra. Such weak repulsions are frequently observed in Nb_6O_{12} clusters (Köhler *et al.*, 1992), in contrast to the corresponding strong repulsions in Nb_6X_{12} clusters when X = Cl, Br. The corresponding average Cl—Nb—Cl angle in, for example, $LuNb_6Cl_{18}$ is thus 164.8° (Ihmaine, Perrin, Pena & Sergent, 1988) and 160.0° for Br—Nb—Br in $K_4Nb_6Br_{18}$ (Veno & Simon, 1985). In the perovskite NbO_6 octahedra the Nb7—O8 distance is significantly longer [2.075 (1) Å] than the Nb7—O7 and Nb7—O9 distances, 1.96 (2) and 2.01 (2) Å, respectively. The elongation of the NbO_6 octahedron along the *c* axis is a result of the slight mismatch in size between the $BaNbO_3$ and NbO parts of the structure. Consequently, the Nb7—O8 distance is rather long for a high-valent Nb atom, which is compensated by the remaining distances being shorter, a condition also observed in other oxoniobate intergrowth structures (Köhler *et al.*, 1992). The Ba—O distances are also similar to those found in other barium oxoniobates, *e.g.* $Ba_{0.95}NbO_3$ (2.889 Å) (Hessen *et al.*, 1991) and $Ba_2Nb_5O_9$ (2.852–2.952 Å) (Svensson *et al.*, 1991). The cubo-octahedron is somewhat distorted, with slightly longer distances to the O atoms of the NbO_6 octahedron, 2.966 (2)–2.997 (2) Å, than to the remaining ones 2.82 (1)–2.90 (1) Å.

The Nb6—Nb6 inter-NbO-block distances, 3.020 (4) Å, are sufficiently short for Nb—Nb bonding between NbO blocks to be considered. However, if significant Nb—Nb bonding between NbO blocks

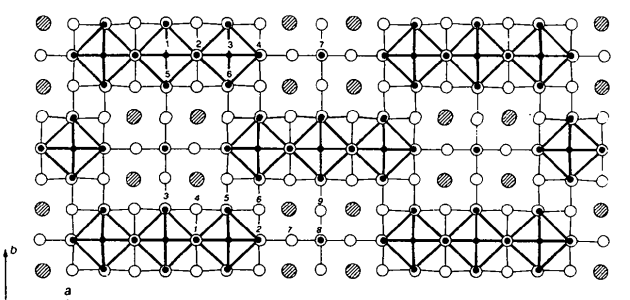

Fig. 4. Structure of $Ba_4Nb_{14}O_{23}$ viewed along [001]: Ba atoms large hatched circles, O atoms large unfilled circles, Nb atoms small filled circles. The numbering of the Nb atoms and O atoms (italics) is given.

were present, one would expect the capping O atoms to be repelled from the bond, as observed in the structure of LT-NbO_2 (Schweizer & Gruehn, 1982). This is not observed in the present case, nor in $BaNb_5O_8$, which contains single NbO columns with an inter-column Nb—Nb distance of 3.041 Å (Zubkov, Perelyaev, Berger, Kontzevaya *et al.*, 1990). Furthermore, extended Hückel calculations in accord with Hoffman (1963) indicate only very weak Nb—Nb inter-NbO-block interactions, both in $Ba_4Nb_{14}O_{23}$ (unpublished results) and in $BaNb_5O_8$ (Köhler *et al.*, 1992).

A calculation of empirical bond valencies (Brown & Altermatt, 1985) from the structural data yields values which, to a certain extent, deviate from expected ones for an ionic model. Similar deviations are, however, observed for other oxoniobate structures with Nb_6O_{12} clusters (Köhler *et al.*, 1992). The Ba atom shows a bond-valence sum of 2.21, the same as observed in $Ba_{0.95}NbO_3$. The O atoms can be divided into two groups; six O atoms with values 2.12–2.43, above the ideal of 2, and three with a lower bond-order sum, 1.85–1.91. The latter three are all located in the NbO_6 octahedra, and the low values reflect the strain introduced by the mutual adjustments of the perovskite and NbO slabs in the structure. The Nb4, Nb5 and Nb6 atoms, pyramidally coordinated by five O atoms, show values between 2.98 and 3.05. The Nb1, Nb2 and Nb3 atoms, coordinated by four O atoms and eight Nb atoms, have the values 2.31–2.42, close to the value 2.41 found for Nb in NbO. The Nb7 atom in the perovskite block has an empirical bond valence of 4.58. This value is decisive for a calculation of the number of electrons involved in Nb—Nb bonding in the NbO block. Formal oxidation numbers of 2 for the Ba atom and 4 for the perovskite Nb7 atom yield 31 metal-cluster electrons. This value coincides with a predicted optimum number of 31 electrons, obtained *via* a counting scheme (Köhler *et al.*, 1992) where three electrons are assigned to the five Nb atoms connecting Nb_6 octahedra and two electrons to the eight remaining Nb atoms. There is, however, a possibility that a charge transfer, δ, occurs from the perovskite block to the NbO block, giving $31 + \delta$ ($0 \le \delta \le 1$) metal-cluster electrons. Bond-order sums and analysis indicate that such a charge transfer occurs in $Sr_2Nb_5O_9$ (Svensson, Köhler & Simon, 1992*b*) and $Ba_2Nb_5O_9$ (Svensson *et al.*, 1991). The observed bond valence and charge transfer are 4.53 and $\delta = 0.47$ for $Sr_2Nb_5O_9$ and 4.32 and $\delta = 0.68$ for $Ba_2Nb_5O_9$. The observed bond valence of 4.58 for the Nb7 atom in $Ba_4Nb_{14}O_{23}$ indicates a δ of the same magnitude as found for $Sr_2Nb_5O_9$. The presence of a charge transfer in the above structures is substantiated by extended Hückel calculations. However, these yield a full charge transfer of $\delta = 1$ for all three structures, implying a five-valent Nb atom in the NbO_6 octahedra, contrary to the partial charge transfer indicated by the bond-valence sums.

In conclusion, the observed bond lengths and bond-valence sums for $Ba_4Nb_{14}O_{23}$ are found to conform well with data for similar oxoniobate intergrowth structures.

The authors wish to thank the Swedish Natural Science Research Council for financial support and also the Philips Application Laboratory in Eindhoven, The Netherlands, for the use of their CM 30 transmission electron microscope.

References

BRAUER, G. (1941). *Z. Anorg. Allg. Chem.* **248**, 1–31.

BROWN, I. D. & ALTERMATT, D. (1985). *Acta Cryst.* **B41**, 244–247.

HAENKO, B. V. & SIVAK, O. P. (1990). *Kristallografiya*, **35**, 1110–1115.

HESSEN, B., SUNSHINE, S. A., SIEGRIST, T., FIORY, A. T. & WASZCZAK, J. V. (1991). *Chem. Mater.* **3**, 528–534.

HESSEN, B., SUNSHINE, S. A., SIEGRIST, T. & JIMENEZ, R. (1991). *Mater. Res. Bull.* **26**, 85–90.

HOFFMAN, R. (1963). *J. Chem. Phys.* **39**, 1397–1412.

IHMAINE, S., PERRIN, C., PENA, O. & SERGENT, M. (1988). *J. Less Common Met.* **137**, 323–333.

KÖHLER, J., SIMON, A., HIBBLE, S. J. & CHEETHAM, A. K. (1988). *J. Less Common Met.* **142**, 123–133.

KÖHLER, J., SVENSSON, G. & SIMON, A. (1992). *Angew. Chem.* **104**, 1463–1483; *Angew. Chem. Int. Ed. Engl.* **31**, 1437–1456.

KREISER, R. R. & WARD, R. (1970). *J. Solid State Chem.* **1**, 368–371.

O'KEEFE, M. A., BUSECK, P. R. & IJIMA, S. (1978). *Nature (London)*, **274**, 322–324.

ROTH, R. S. & WARING, J. L. (1961). *J. Res. Natl Bur. Stand. Sect. A*, **65**, 337–344.

SCHÄFER, H. & SCHNERING, H.-G. (1964). *Angew. Chem.* **76**, 833–868.

SCHWEIZER, H. J. & GRUEHN, R. (1982). *Z. Naturforsch. Teil* B, **37**, 1361–1368.

SHELDRICK, G. M. (1976). *SHELX*76. Program for crystal structure determination. Univ. of Cambridge, England.

SVENSSON, G. (1988). *Mater. Res. Bull.* **23**, 437–446.

SVENSSON, G. (1990). *Microsc. Microanal. Microstruct.* **1**, 343–356.

SVENSSON, G., KÖHLER, J., OTTEN, M. T. & SIMON, A. (1993). *Z. Anorg. Allg. Chem.* **619**, 133–137.

SVENSSON, G., KÖHLER, J. & SIMON, A. (1991). *J. Alloys Comp.* **176**, 123–133.

SVENSSON, G., KÖHLER, J. & SIMON, A. (1992*a*). *Angew. Chem.* **104**, 192–193; *Angew. Chem. Int. Ed. Engl.* **31**, 212–213.

SVENSSON, G., KÖHLER, J. & SIMON, A. (1992*b*). *Acta Chem. Scand.* **46**, 244–248.

VENO, F. & SIMON, A. (1985). *Acta Cryst.* C**41**, 308–310.

ZUBKOV, V. G., PERELYAEV, V. A., BERGER, I. F., KONTSEVAYA, I. A., MAKAROVA, O. V., TURZHEVSKII, S. A., GUBANOV, V. A., VORONIN, A. V., MIRMILSTEIN, V. I. & KAR'KIN, A. E. (1990). *Sverkhprovod. Fiz. Khim. Tekh.* **3**, 2121–2127.

ZUBKOV, V. G., PERELYAEV, V. A., BERGER, I. F., VORONIN, V. I., KONTSEVAYA, I. A. & SHVEIKIN, G. P. (1990). *Dokl. Akad. Nauk SSSR*, **312**, 615–618.

ZUBKOV, V. G., PERELYAEV, V. A., TYUTYUNNIK, A. P., KONTSEVAYA, I. A., MAKAROVA, O. V. & SHVEIKIN, G. P. (1992). *Dokl. Akad. Nauk Russ.* **325**, 740–745.

ZUBKOV, V. G., PERELEYAEV, V. A., TYUTYUNNIK, A. P., KONTSEVAYA, I. A., VORONIN, V. I. & SVENSSON, G. (1993). In preparation.